Research paper

How does varying water supply affect oxygen isotope variations in needles and tree rings of Scots pine?

Galina Timofeeva[1,2,3], Kerstin Treydte[2], Harald Bugmann[3], Yann Salmon[4,5], Andreas Rigling[2], Marcus Schaub[2], Pierre Vollenweider[2], Rolf Siegwolf[1,2] and Matthias Saurer[1,2,6]

[1]Laboratory of Atmospheric Chemistry, Paul Scherrer Institute (PSI), Villigen 5232, Switzerland; [2]Research Unit Forest Dynamics, Swiss Federal Institute for Forest, Snow and Landscape Research WSL, Birmensdorf 8903, Switzerland; [3]Forest Ecology, Institute of Terrestrial Ecosystems, ETH Zurich, Zurich 8092, Switzerland; [4]Department of Physics, University of Helsinki, Helsinki 00014, Finland; [5]School of GeoSciences, University of Edinburgh, Edinburgh EH9 3FF, UK; [6]Corresponding author (matthias.saurer@wsl.ch)

In many regions, drought is suspected to be a cause of Scots pine decline and mortality, but the underlying physiological mechanisms remain unclear. Because of their relationship to ecohydrological processes, $\delta^{18}O$ values in tree rings are potentially useful for deciphering long-term physiological responses and tree adaptation to increasing drought. We therefore analyzed both needle- and stem-level isotope fractionations in mature trees exposed to varying water supply. In a first experiment, we investigated seasonal $\delta^{18}O$ variations in soil and needle water of Scots pine in a dry inner Alpine valley in Switzerland, comparing drought-stressed trees with trees that were irrigated for more than 10 years. In a second experiment, we analyzed twentieth-century $\delta^{18}O$ variations in tree rings of the same forest, including a group of trees that had recently died. We observed less ^{18}O enrichment in needle water of drought-stressed compared with irrigated trees. We applied different isotope fractionation models to explain these results, including the Péclet and the two-pool correction, which considers the ratio of unenriched xylem water in the needles to total needle water. Based on anatomical measurements, we found this ratio to be unchanged in drought-stressed needles, although they were shorter. The observed lower ^{18}O enrichment in needles of stressed trees was therefore likely caused by increased effective path length for water movement within the leaf lamina. In the tree-ring study, we observed lower $\delta^{18}O$ values in tree rings of dead trees compared with survivors during several decades prior to their death. These lower values in declining trees are consistent with the lower needle water ^{18}O enrichment observed for drought-stressed compared with irrigated trees, suggesting that this needle-level signal is reflected in the tree rings, although changes in rooting depth could also play a role. Our study demonstrates that long-term effects of drought are reflected in the tree-ring $\delta^{18}O$ values, which helps to provide a better understanding of past tree physiological changes of Scots pine.

Keywords: climate change, *Pinus sylvestris*, post-photosynthetic fractionation, stable isotopes, tree mortality.

Introduction

Water is a key factor for plant growth and survival, and hence, understanding the variability in plant water uptake and transpiration is of paramount importance. This becomes even more pertinent in regions where plants experience acute or chronic drought that may lead to tree mortality (Allen et al. 2010, 2015, Choat et al. 2012, Anderegg et al. 2013). Understanding plant and particularly tree response to drought is a pressing issue in view of climate change, having triggered many studies (McDowell et al. 2008, Breshears et al. 2013). However, most experimental studies were performed with seedlings and saplings of various tree species (Galle et al. 2010, Pearson et al. 2013, Duan et al. 2015, Cocozza et al. 2016) and only rarely with mature trees (Galiano et al. 2010, Poyatos

et al. 2013, Aguadé et al. 2015, Gaylord et al. 2015, Salmon et al. 2015). Therefore, drought manipulation studies in natural environments are crucial to further develop our understanding of the physiological responses of mature trees to drought, including associated isotope fractionations (Herzog et al. 2014, Rowland et al. 2015, Grossiord et al. 2018).

Stable oxygen isotope ratios (expressed as $\delta^{18}O$ values) in plant organic matter have already been used to investigate ecophysiological and ecohydrological responses during drought (Moreno-Gutiérrez et al. 2012, Sargeant and Singer 2016). It is known that $\delta^{18}O$ values of meteoric water are variable due to large-scale hydrological processes and temperature effects (Dansgaard 1964, Craig and Gordon 1965). These variations are reflected in soil water, with modification through mixing and evaporation. The soil water is taken up by plant roots without fractionation (Ehleringer and Dawson 1992), but in the leaves the isotope ratio is further changed owing to equilibrium and kinetic fractionation processes during transpiration (Dongmann et al. 1974, Farquhar et al. 2007) and carbohydrate production (Roden and Ehleringer 1999, Lehmann et al. 2017). Therefore, $\delta^{18}O$ variations in plant organic matter such as tree rings are characterized by a complex, mixed isotope signal arising from the source water, the evaporative leaf water ^{18}O enrichment, and biochemical source-to-sink isotope fractionations (Gessler et al. 2014).

Although $\delta^{18}O$ values in tree rings have often been used to reconstruct past environmental conditions (Libby et al. 1976, Masson-Delmotte et al. 2005, Treydte et al. 2006, Edwards et al. 2008, Rinne et al. 2013, Labuhn et al. 2016), these studies mainly relied on statistical relationships with climate variables and thus may not always adequately account for all processes (McCarroll and Loader 2004, Treydte et al. 2014). It would be important to apply mechanistic, process-based models for better understanding of the factors controlling the isotope fractionation in foliage and tree rings related to various environmental conditions, including drought. The mechanistic Craig–Gordon model has often been applied to this end, mostly at the leaf level (Craig and Gordon 1965, Farquhar and Lloyd 1993). It has been critically discussed that this model often overestimates leaf water ^{18}O enrichment and thus needs a correction for improved accuracy (Barbour 2007, Ogée et al. 2007). To date, there is no general correction approach suitable across different species. In many studies, the so-called Péclet correction was applied, requiring sometimes rather unrealistic adjustments of its parameters (Ferrio et al. 2012, Song et al. 2013, Cernusak et al. 2016). Therefore, it has been suggested that the so-called two-pool correction could be more adequate, particularly for conifers (Roden et al. 2015, Song et al. 2015, Bögelein et al. 2017), or a combination of the two-pool model and Péclet correction (Holloway-Phillips et al. 2016). Additionally, current mechanistic models have been challenged by the limited understanding of post-photosynthetic isotope

fractionation and the biochemical processes responsible for the incorporation of the cellulose oxygen isotopic signature into tree rings (Waterhouse et al. 2002, Gessler et al. 2009, 2014, Ogée et al. 2009, Sternberg 2009, Cheesman and Cernusak 2017). During drought, various changes act in combination, such as temperature, source water composition, vapor pressure deficit (VPD), stomatal conductance and needle morphological properties. Therefore, it remains difficult to disentangle these factors and use $\delta^{18}O$ in tree rings as a proxy for reconstructing long-term environmental changes or for better understanding of the causes of tree mortality.

In this study, we investigated a drought-stressed Scots pine population from one of the driest parts of the European Alps (Valais, Switzerland), which has been subjected to a long-term irrigation experiment since 2003. In a first experiment, we measured $\delta^{18}O$ values in water extracted from different soil depths and needles of drought-stressed and irrigated trees sampled multiple times between 2013 and 2015. In a second experiment at the same site, we analyzed the $\delta^{18}O$ values in tree-ring cellulose from Scots pine trees that had recently died and compared them with the signal from living trees over the period 1900–2014. Our first aim was to identify the factors controlling leaf-level isotope fractionation of Scots pine under drought and irrigation, considering evaporative leaf water enrichment, gas-exchange and needle morphological properties. Particularly, the basic Craig–Gordon model and Péclet and the two-pool correction were explored. Our second aim was to disentangle the effects of climate and tree physiology on long-term variations in $\delta^{18}O$ by comparing measured tree-ring $\delta^{18}O$ values with predicted ones using a fractionation model corrected with a similar approach as for needles. This should help to determine the driving factors of tree-ring oxygen isotope variability in drought-stressed Scots pine trees.

Materials and methods

Study site

The study was carried out in the Pfynwald forest (46° 18′ N, 7° 36′ E, 615 m above sea level (a.s.l.)) in Valais, Switzerland. The site is a natural Scots pine (*Pinus sylvestris* L.) forest located in one of the driest inner Alpine valleys of the European Alps, where severe Scots pine decline and mortality have already been observed (Bigler et al. 2006, Rigling et al. 2013). The forest is characterized as uneven-aged Erico-Pinetum sylvestris with shallow soil and low water retention (Dobbertin et al. 2010). Because of the blockage of moisture incoming from oceanic air masses by the high surrounding mountain ranges, the climate in Central Valais is continental. For the 1981–2010 period, mean annual precipitation was 605 mm, with 169 mm only during summer, while the mean annual temperature was 10.1 °C (19.1 °C for summer). In 2003, an irrigation experiment was initiated at this site (Dobbertin et al. 2010, Eilmann et al.

2010, Herzog et al. 2014), consisting of four drought-stressed and four irrigated plots of 1000 m² each. The irrigation water was taken from a river channel near the experimental area, and irrigation took place every growing season between April and October. The irrigated trees received approximately twice the amount of total annual precipitation compared with the drought-stressed trees, i.e., ca 1300 mm.

Sampling, sample preparation and measurements

To measure seasonal $\delta^{18}O$ variations in needle water, one tree per plot (i.e., four drought-stressed trees and four irrigated trees) was selected for repeated samplings between August 2013 and August 2015. Sampling was conducted every month from June to August and approximately every second month for the other periods. Several twigs were cut at a height of 10–12 m from the sun-exposed part of the crown using a pole pruner. Current-year needles were immediately separated from twigs, stored in airtight glass vials with screw caps, and placed in the dark in a cooling box with ice packs to minimize evaporative water loss.

At the same sampling dates, soil samples from each plot (four per treatment) were collected at two depths (0–10 and 10–20 cm) and stored in airtight glass vials to monitor seasonal $\delta^{18}O$ variations of the soil water. Deeper sampling depths were generally not accessible due to the rocky soil. However, there was one soil profile down to 80 cm available, where soil samples were excavated on 9 April 2014. Water samples from the channel (irrigation source) were collected at each sampling date as well. Increment cores from the four drought-stressed and four irrigated trees were sampled for stem water extraction in August and October 2014 (one 0.5 cm core per tree). Because xylem water was not systematically collected during the experiment in 2013–15, twig phloem, twig xylem and stem xylem samples during August 2017 were taken to confirm the difference in source water between drought-stressed and irrigated trees.

Water from soil, needles and tree increment cores were obtained using a cryogenic vacuum extraction system (West et al. 2006, Saurer et al. 2016). In brief, glass vials with samples were placed in a water bath at 80 °C. The evaporated water from samples was collected into U-shaped glass tubes that were cooled down with liquid nitrogen. Both glass vials with samples and tubes were connected to a vacuum system at ca 4×10^{-2} mbar. Subsequently, the extracted water samples were transferred into 2 ml sealed glass vials. The $\delta^{18}O$ values of these water samples were measured by injecting 0.6 µl of the sample into a thermal conversion elemental analyzer (TC/EA; Thermo Finnigan, Bremen, Germany), where the water was pyrolyzed in a glassy carbon reactor at 1450 °C to hydrogen (H_2) and carbon monoxide (CO). These gases were carried in a helium stream to an isotope ratio mass spectrometer (IRMS) Delta Plus XP (Thermo Finnigan) for $\delta^{18}O$ analysis. The results were reported in the standard δ-notation as per mil (‰) relative to the Vienna Standard Mean Ocean Water, with a precision of <0.2‰.

Twelve stem disks of standing dead trees (subsequently called 'now-dead/dead trees') and increment cores from 32 trees ('now-living/living trees') were sampled within the non-irrigated (drought-stressed/ambient) area. Tree-ring widths (TRW) were measured at the tree-ring laboratory of the Swiss Federal Institute for Forest, Snow and Landscape Research WSL in Birmensdorf, Switzerland. The chronologies of the dead and living trees cover the period of 1900–2005 and 1900–2014, respectively. For details on sampling, sample preparation, and TRW measurements, see Timofeeva et al. (2017). For $\delta^{18}O$ measurements, the tree rings were separated according to calendar year, and cellulose was extracted following Leavitt and Danzer (1993) and Boettger et al. (2007), with modifications according to Roden et al. (2009), and homogenized with an ultrasonic device (Laumer et al. 2009). Aliquots were packed into silver capsules for isotope analyses, which were conducted using a pyrolysis method at 1420 °C in an elemental analyzer (PYRO-cube, Elementar, Hanau, Germany) connected to an isotope ratio mass spectrometer (IRMS, Delta Plus XP) via a ConFlo III interface (Thermo Fischer Scientific, Bremen, Germany) (Weigt et al. 2015). In general, the measurement precision was better than 0.2‰.

Needle gas exchange and anatomical measurements

Leaf gas exchange and net photosynthesis (A_N) and transpiration (E) of five sun-exposed twigs per tree (four irrigated trees, four drought-stressed trees) were measured in June 2013 and May and June 2014. Measurements were performed using a portable photosynthesis system equipped with a 6400-22L leaf chamber (LI-COR 6400Xt; LI-COR, Lincoln, NE, USA). Conditions in the cuvette were kept constant during the measurements at 400 p.p.m. [CO_2] and a photon flux density of 1000 µmol m^{-2} s^{-1}, while the temperature was adjusted close to ambient conditions. Initial leaf–gas exchange values were corrected a posteriori for the exact projected leaf area according to Fleck et al. (2016).

To measure the needle length of current-year needles, 10 trees at the drought-stressed and 12 trees at the irrigated plots were selected. Measurements were repeated every year during summer from 2013 to 2015. For the anatomical assessments of needles, one branch from the sun crown of five trees per experimental plot was pole-pruned in February 2015. Needle samples from the last three needle generations were fixed in 2.5% glutaraldehyde buffered at pH 7.0 with a 0.067 M Sorensen phosphate buffer and stored at 4 °C until processing (here, we only present data for the 2013 and 2014 needle generations). The size of tissues and histological composition were assessed using 70 µm hand-microtomed cross sections from the hydrated middle part of needles. The cuttings were visually analyzed with bright-field microscopy using the 10×

objective of a Leica microscope Leitz DMRB and imaged using the Lumenera Infinity 2.1R camera and Lumenera Infinity Analyze (release 6.4) software (Lumenera Corp., Ottawa, Canada). The total area of needle cross sections and that of each tissue (epidermis; hypodermis; resin ducts; mesophyll; endodermis; transfusion tissues; phloem; xylem) was determined by means of image analysis and the measurement tools in the Adobe Photoshop software (Cs5, version 12.0.0.0; Adobe Systems Inc., San Jose, CA, USA), using stitched micrographs. The histological composition was calculated by expressing each tissue in percentage area of the whole needle section.

Oxygen isotope modeling

As a first approximation, the needle water isotope ratio ($\delta^{18}O_N$) in the steady state can be calculated by the Craig and Gordon (1965) equation modified by Dongmann et al. (1974):

$$\delta^{18}O_N = \delta^{18}O_{SW} + \varepsilon^+ + \varepsilon_k + \left(\delta^{18}O_V - \delta^{18}O_{SW} - \varepsilon_k\right) \cdot e_a/e_i \tag{1}$$

where $\delta^{18}O_{SW}$ is the isotope value of the source water (xylem), ε^+ is the equilibrium fractionation related to the phase change from liquid to vapor, ε_k is the kinetic fractionation related to the diffusion in air, $\delta^{18}O_V$ is the atmospheric water vapor isotope value, and e_a/e_i is the ratio of leaf external (ambient) to internal water vapor pressures.

To exclusively characterize the isotope fractionation within the leaf without influences of the source water isotope variation, the leaf water enrichment term $\Delta^{18}O_N$ is often used, which is obtained after subtracting $\delta^{18}O_{SW}$ from $\delta^{18}O_N$:

$$\Delta^{18}O_N = \varepsilon^+ + \varepsilon_k + \left(\delta^{18}O_V - \delta^{18}O_{SW} - \varepsilon_k\right) \cdot e_a/e_i \tag{2}$$

We refer to this equation as the CG model ('Craig–Gordon model'). The equilibrium fractionation (ε^+) depends on temperature and can be calculated according to Bottinga and Craig (1968):

$$\varepsilon^+ (‰) = 2.664 - 3.206 \cdot 10^3/T + 1.534 \cdot 10^6/T^2 \tag{3}$$

The kinetic fractionation (ε_k) has an approximate value of 28‰ (Cernusak et al. 2016). The e_a/e_i ratio can be simplified using relative air humidity (RH) for the calculations, assuming that RH inside the leaf is 100% and that leaf and air temperatures are equal, although this may not always be the case, particularly for sun-exposed needles or leaves. Parts of Eqs (1) and (2), i.e., $\delta^{18}O_V - \delta^{18}O_{SW}$, can be replaced by $-\varepsilon^+$, assuming isotopic equilibrium between soil (source) water and water vapor (Foerstel and Huetzen 1983, Bögelein et al. 2017).

Eq (1) and (2) were found to predict the variability of observed leaf water ^{18}O enrichment reasonably well (Farquhar and Lloyd 1993, Roden and Ehleringer 1999, Cernusak et al. 2016), but they often overestimate actual values. Therefore, a model correction based on the Péclet effect was proposed

(Farquhar and Lloyd 1993, Barbour 2007, Cernusak et al. 2016). It can be characterized by the Péclet number $\wp$ and considers an isotopic gradient between xylem and evaporative sites, which is mainly driven by changes in transpiration (E) and the so-called effective path length (L):

$$\wp = L \cdot E/(C \cdot D) \tag{4}$$

where L (m) describes the tortuous path that water travels from the leaf veins to the sites of evaporation, E is the transpiration rate (mmol m^{-2} s^{-1}), C is the molar density of water (55.56×10^3 mol m^{-3}), and D is the diffusivity of H$_2$^{18}O in water, which depends on temperature (Cuntz et al. 2007, Cernusak et al. 2016). However, the effective path length (L) is not a directly measurable parameter and difficult to quantify. Mostly, as in our study, it is determined by an iterative procedure to minimize the square root of the sum of all differences between measured and modeled values (Barbour et al. 2004).

Leaf ^{18}O enrichment after the Péclet correction is then given as

$$\Delta^{18}O_N{}^* = \Delta^{18}O_N \cdot \left(1 - e^{-\wp}\right)/\wp \tag{5}$$

Furthermore, a two-pool model was suggested as a correction for the CG model (Yakir et al. 1990, Song et al. 2015, Cernusak et al. 2016). It assumes that total needle water is a mixture of two discrete pools of water, i.e., unenriched water influenced mainly by xylem water (the central part of the needle consisting of the endodermis, xylem, phloem and transfusion tissues) and ^{18}O-enriched water at the evaporative sites (mainly the mesophyll tissue), as follows:

$$\Delta^{18}O_N{}^* = \Delta^{18}O_N \cdot (1 - \varphi) \tag{6}$$

where φ is the ratio of unenriched to total needle water (Song et al. 2015, Cernusak et al. 2016) and can be experimentally determined from needle anatomical measurements (Roden et al. 2015). This ratio φ can have a value between 0 (infinitely small xylem contribution) and 1 (xylem water fully dominates the $^{18}O/^{16}O$ ratio of needle water).

The two correction approaches can be combined, i.e., the Péclet correction is applied on the ^{18}O-enriched part of the leaf water only (Holloway-Phillips et al. 2016):

$$\Delta^{18}O_N{}^* = (1-\varphi)\,\Delta^{18}O_N \cdot \left(1 - e^{-\wp}\right)/\wp \tag{7}$$

A modified version of Eq. (1) can then be used to predict ^{18}O enrichment in tree rings:

$$\delta^{18}O_{TR} = \delta^{18}O_{SW} + (1-x) \cdot \Delta^{18}O_N{}^* + \varepsilon_{wc} \tag{8}$$

where $\delta^{18}O_{TR}$ is the predicted tree-ring isotope ratio; ε_{wc} is the biochemical exchange between the oxygen atoms of xylem water and those of the cellulose carbonyl groups, equaling

27‰ (DeNiro and Epstein 1981, Sternberg et al. 1986); and x is the proportion of oxygen atoms of carbonyl groups (e.g., of trioses) undergoing exchange with xylem (stem) water during cellulose formation ($x = 0.42$). The value of x could vary as a function of the turnover of non-structural carbohydrates (Song et al. 2014) and environmental conditions (Cheesman and Cernusak 2017). This can also be expressed as a dampening f of the leaf water signal as reflected in the tree ring $f = 1 - x = 0.58$ (Saurer et al. 1997, Roden et al. 2000, Treydte et al. 2014). As a surrogate for source water ($\delta^{18}O_{sw}$) variations over the investigated period, we used the averages of summer months of $\delta^{18}O$ in precipitation. The validity of this assumption was tested by comparison of measured soil $\delta^{18}O$ values with monthly $\delta^{18}O$ of precipitation (in Results). The needle water enrichment term $\Delta^{18}O_N*$ in Eq. (8) can be expressed with the simple leaf CG model (Eq. (2)), resulting in what we subsequently call the 'tree-ring CG model,' or using the more advanced expression from Eq. (7), resulting in the 'full tree-ring model'.

Climate data

For modeling of needle water ^{18}O enrichment, we used air temperature and relative humidity data from Pfynwald with 10 min resolution for the period of 2013–15. These data were obtained from Sensirion SHT-21 sensors with a multiple-plate radiation shield (± 0.3 °C and $\pm$ 2% RH accuracy). Monthly climate data for 1900–2014 were obtained from the Sion meteorological station (MeteoSwiss archives). The Standardized Precipitation Evapotranspiration Index (SPEI), a multiscalar drought index, was used for correlation analysis with tree-ring parameters (Timofeeva et al. 2017). Monthly $\delta^{18}O$ data of precipitation were obtained from the Global Network of Isotopes in Precipitation (GNIP) and from the Federal Office of Water and Geology, Bern, Switzerland (FOWG). The GNIP data from the Grimsel station (46.57 N, 8.33 E, 1950 m a.s.l.) for the period 1972–2014 were used for tree-ring $\delta^{18}O$ modeling. They were corrected for the elevational offset, using data from the Sion station for the period 1994–2014. To this end, we first calculated averages for each month for this period at both stations and used their differences for the correction. The raw data from the Sion station were not used for tree-ring modeling due to the short observation period.

Data analysis

We determined the response of $\delta^{18}O$ variations to climate by calculating Pearson's correlation coefficients between the monthly mean series of each climate variable (air temperature, precipitation, relative humidity, drought index and vapor pressure deficit (VPD)) and $\delta^{18}O$ for individual months and seasons such as spring (March–May) and summer (June–August). We tested the significance of the correlation coefficients by applying two-tailed Student's t-tests.

Temporal autocorrelation was taken into account by calculating the 'effective' sample size, which is based on sample size and the first-order autocorrelation for each time series and climate data:

$$N' = N \cdot \frac{(1 - r_1 \cdot r_2)}{(1 + r_1 \cdot r_2)} \qquad (10)$$

where N is sample size, N' is effective sample size, and r_1 and r_2 are the first-order sample autocorrelation of the first and second time series, respectively (Dawdy 1964). Two-tailed Student's t-tests were applied to test for significant differences between groups. Two-factor ANOVA was carried out to test for treatment and needle generation differences in needle anatomical data, including a Tukey's HSD post hoc test.

Results

Seasonal variations in $\delta^{18}O$ of needle and soil water

The $\delta^{18}O$ values of needle water strongly fluctuated between sampling dates, showing seasonal differences with values up to ca 10‰ during spring and summer and negative values during winter (Figure 1a). Soil water $\delta^{18}O$ also featured a seasonal pattern at both measured soil depths, but with values always below zero (Figure 1b and c). The $\delta^{18}O$ values of the channel water (source of irrigation) did not show significant seasonal changes and were depleted compared with soil water during the growing season (Figure 1b and c; $P > 0.05$). This depletion resulted in soil water $\delta^{18}O$ values of the irrigated plots to be clearly lower compared with the drought-stressed plots for both soil depths (significant for August 2013 and April 2014, $P < 0.05$). Isotope values at soil depths from 0 to 10 cm were generally enriched in ^{18}O compared with those at soil depths from 10 to 20 cm during spring and summer (except for summer 2014). This strong enrichment of water near the soil surface was consistent with the results of the deep soil profile taken on 9 April 2014 (see Figure S1 available at Supplementary Data at *Tree Physiology* Online). This profile showed that below a depth of 20 cm, there was less variation in the isotopic composition. Furthermore, stem water collected in August and October 2014 showed $\delta^{18}O$ values close to soil water values from 20 cm depth rather than from top soil. Twig phloem, twig xylem and stem xylem samples taken after our experiment, while irrigation was still ongoing (August 2017), confirm the ^{18}O depletion of water taken up by irrigated trees compared with drought-stressed trees (see Figure S2 available at Supplementary Data at *Tree Physiology* Online). Considering all this information, the soil depth 10–20 cm was considered representative for the depth from where the source water was mainly taken up.

Needle water $\delta^{18}O$ values did not show any significant differences between drought-stressed and irrigated trees ($P > 0.05$). However, it is important to consider that soil water $\delta^{18}O$ values of the irrigated plots were clearly lower compared with the
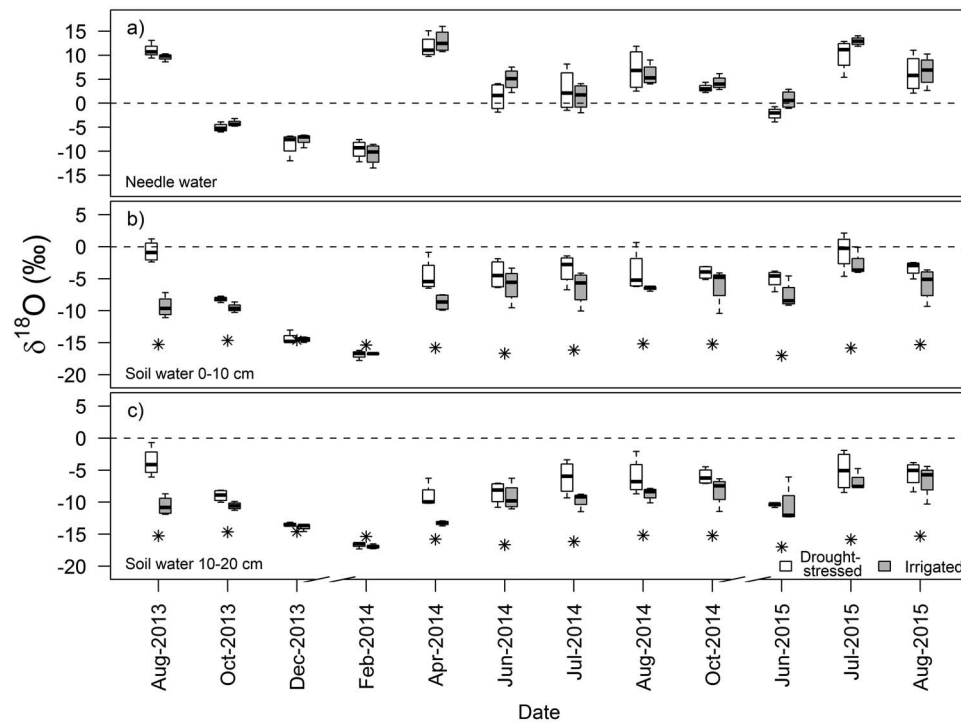
Figure 1. Seasonal variations in $\delta^{18}O$ of needle water (a), and soil water at 0–10 cm (b), and at 10–20 cm (c) shown for drought-stressed and irrigated plots. Isotope values of channel water used for irrigation are displayed as stars (b, c).

drought-stressed plots due to lower $\delta^{18}O$ values in the channel water used for irrigation. Accordingly, calculated needle water enrichment above source water ($\Delta^{18}O$) based on the difference between $\delta^{18}O$ of needle water and water of soil depths 10–20 cm was higher for irrigated trees compared with the drought-stressed trees at almost all sampling points (Figure 2). This divergence was most pronounced during spring and summer, although significant differences between drought-stressed and irrigated trees were only observed for August 2013 and April 2014 ($P < 0.05$), but not for the summer months of 2014 and 2015.

Gas exchange and needle properties

Transpiration rate per leaf area was on average higher for the irrigated compared with the drought-stressed trees, except for the sampling in June 2013 (Table 1). However, differences between treatments were only marginally significant ($P < 0.1$), whereas they were significant for the combined data of all tree in the treatment for both samplings in 2014 ($P < 0.01$) and for the combined sampling dates over the period of 2013–14 ($P < 0.05$). These data were used to establish a linear relationship between E and VPD, which explained more than 60% of the variability in E and yielded a slope of 0.11 mmol m^{-2} s^{-1} hPa^{-1} for drought-stressed and 0.19 mmol m^{-2} s^{-1} hPa^{-1} for irrigated trees. This relationship was subsequently used to estimate E on dates without gas-exchange measurements needed for leaf water modeling.
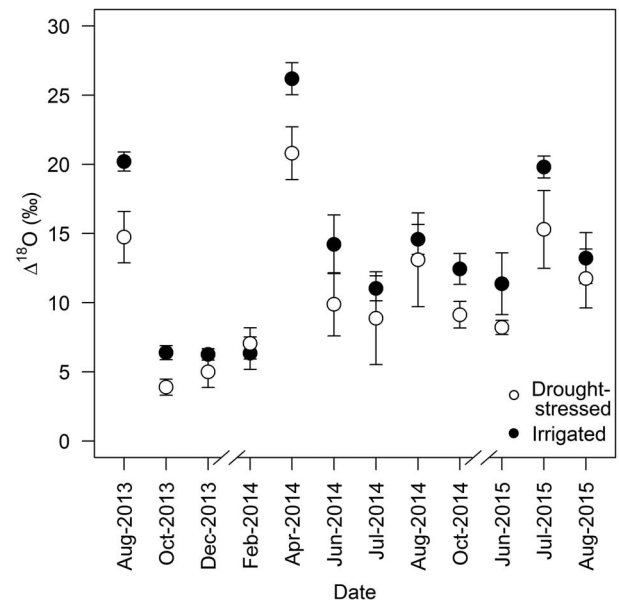

Figure 2. Seasonal changes in needle water ^{18}O enrichment ($\Delta^{18}O$) calculated as difference between needle water $\delta^{18}O$ and soil water at 10–20 cm.

Needles of the drought-stressed trees were shorter (on average 34.67 mm) compared with those of the irrigated trees (on average 44.31 mm), with a high variability for both treatments (Table 2). Differences in needle length between

Table 1. Transpiration rates for the period of 2013–14. Numbers are mean values of four trees ± SD. NA, not available (only one tree measured).

Date	Transpiration rate (mmol m⁻² s⁻¹)	
	Drought-stressed	Irrigated
18 June 2013	0.35 ± 0.08	0.36 ± 0.17
06 May 2014	0.22 ± 0.07	1.01 ± NA
03 June 2014	0.12 ± 0.05	0.21 ± 0.05
2013–14	0.24 ± 0.12	0.43 ± 0.34

Table 2. Needle length data determined during summer 2013 and 2014. Numbers are mean values (±SD) of 10 drought-stressed and 12 irrigated trees.

Date	Needle length (mm)	
	Drought-stressed	Irrigated
2013	38.77 ± 7.61	48.24 ± 7.27
2014	30.57 ± 8.57	40.38 ± 8.45
2013–14	34.67 ± 8.94	44.31 ± 8.69

drought-stressed and irrigated trees were significant both for the averaged and for all measured values for 2013 ($P < 0.01$), 2014 ($P < 0.05$) and over the period of 2013–14 ($P < 0.001$).

The cross-sectional area of the different needle tissues all showed a significant difference between the two needle generations (ANOVA, $P < 0.01$; Table 3). Treatment (i.e., drought-stressed vs irrigated) was significant for resin, transfusion tissues, phloem and xylem, while no interaction between needle generation and treatment was found. Differences in total needle cross section between the drought-stressed and irrigated trees were not significant. We estimated the proportion of tissue not subjected to evaporative ¹⁸O enrichment φ as the ratio of the sum of endodermis, xylem, phloem and transfusion tissues to total needle cross section. This proportion amounted to 0.270 ± 0.014 for drought-stressed and 0.282 ± 0.013 for irrigated trees averaged over both needle generations. These values were used in the subsequent model calculations.

Modeling needle water ¹⁸O enrichment

We found a highly significant correlation between measured and CG-modeled needle water ¹⁸O enrichment values using the basic equation (Eq. (2), Figure 3). However, modeled values were only accurate for winter conditions, when ¹⁸O enrichment was low, but they were strongly overestimated for both treatments (by up to 10‰) during summer months (Figure 3, Table 4). Accordingly, slopes of the linear regression strongly deviated from 1 (Figure 3a, drought-stressed trees: slope = 0.44, R^2 = 0.66, $P < 0.01$; irrigated trees: slope = 0.53, R^2 = 0.62, $P < 0.01$). Furthermore, the basic CG model could not explain the observed difference in

Table 3. Average cross-sectional areas of different tissues (±SD) for both treatments and two needle generations as well as the proportion of not ¹⁸O-enriched tissue ('non-enriched'). Non-enriched is defined as the sum of endodermis, xylem, phloem and transfusion tissues.

| Treatment	Needle generation	Needle (mm²)	Epidermis + hypodermis (mm²)	Resin ducts (mm²)	Mesophyll (mm²)	Endodermis (mm²)	Transfusion tissues (mm²)	Phloem (mm²)	Xylem (mm²)	Non-enriched/total
Drought-stressed	2013	0.868 ±0.137	0.128 ±0.016	0.091 ±0.017	0.415 ±0.067	0.040 ±0.007	0.166 ±0.036	0.020 ±0.004	0.008 ±0.002	0.269 ±0.015
Irrigated	2013	0.900 ±0.187	0.132 ±0.019	0.097 ±0.026	0.417 ±0.095	0.040 ±0.006	0.180 ±0.042	0.024 ±0.007	0.012 ±0.004	0.283 ±0.013
Drought-stressed	2014	0.694 ±0.131	0.110 ±0.017	0.074 ±0.015	0.322 ±0.065	0.031 ±0.005	0.138 ±0.031	0.013 ±0.003	0.006 ±0.002	0.271 ±0.014
Irrigated	2014	0.810 ±0.211	0.121 ±0.023	0.088 ±0.026	0.373 ±0.106	0.036 ±0.007	0.166 ±0.049	0.016 ±0.005	0.010 ±0.003	0.281 ±0.012
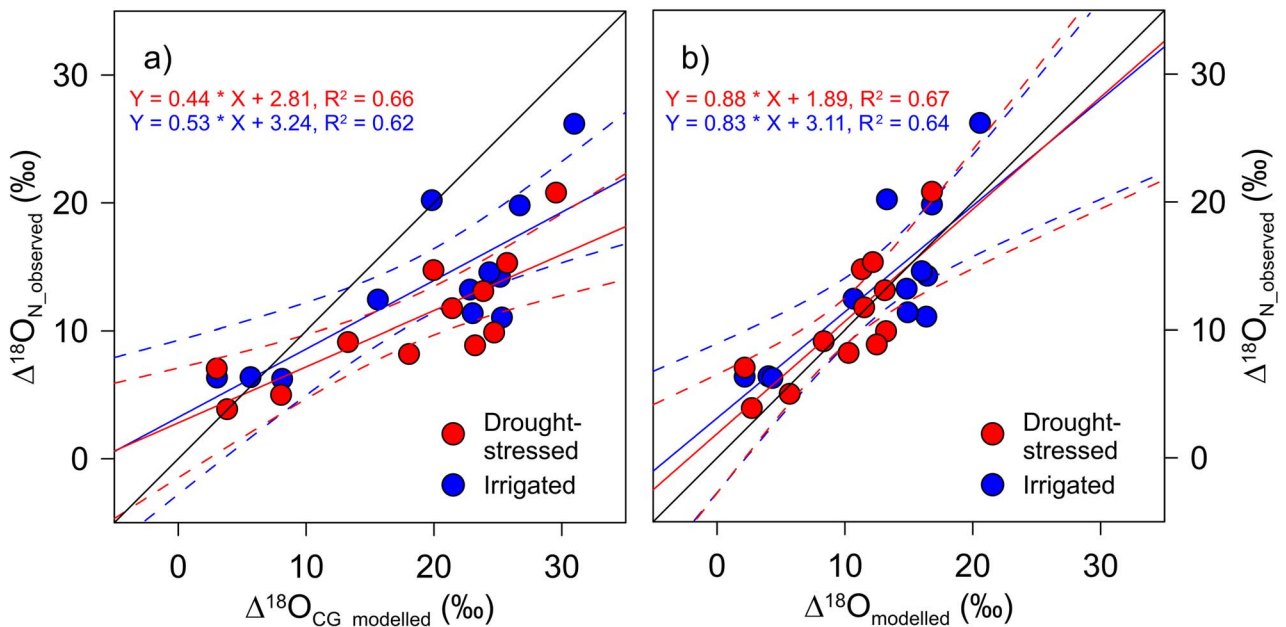
Figure 3. Relationship between measured and predicted needle water ^{18}O enrichment using the basic Craig–Gordon model (Eq. (2), a) and the full model with the combined Péclet and two-pool correction (Eq. (7), b). Regression lines and equations are also indicated. The dashed lines show 95% confidence intervals.

^{18}O enrichment between treatments. Results obtained from the model incorporating the Péclet- and two-pool corrections (Eq. (7)) reflected the variability of the data much better, as the linear regression slopes were closer to 1 (Figure 3b, drought-stressed trees: slope $= 0.88$, $R^2 = 0.67$, $P < 0.01$; irrigated trees: slope $= 0.83$, $R^2 = 0.64$, $P < 0.01$). Furthermore, average growing season values calculated with this model were very close to measured ^{18}O enrichment for both treatments, and the difference between treatments of about 3.5‰ was well reproduced (Table 4). These calculations were based on φ derived from anatomical measurements and L optimized for minimum deviation from the data (Barbour et al. 2004). This resulted in high L of 0.32 and 0.05 m for drought-stressed and irrigated groups, respectively. Even higher values of L of 0.7 and 0.25 m would have resulted if neglecting the two-pool model (i.e., $\varphi = 0$). Due to the high L, the Péclet effect ($\wp$) was overall stronger for drought-stressed trees, despite the lower transpiration (Table 4), resulting in the lower ^{18}O enrichment observed compared with irrigated trees.

Tree-ring $\delta^{18}O$ values and their relationship to climate

The mean tree-ring $\delta^{18}O$ chronologies calculated from the five living and five now-dead trees, respectively, were highly correlated for the common period (Figure 4a, 1900–2004, $r = 0.76$, $P < 0.001$), but also the mean inter-series correlations of the individual tree series for both groups where highly significant (see Figures S3 and S4 available at Supplementary Data at Tree Physiology Online). The tree-ring $\delta^{18}O$ chronologies of the living and the now-dead trees did not show any significant

Table 4. List of parameters and leaf water model results calculated as average of all sampling days during the growing seasons (omitting October–February data). The equilibrium fractionation ε^+ is calculated according to Eq. (3), the diffusivity D according to Cuntz et al. (2007), the path length L obtained through optimization (see text for details), the Péclet number $\wp$ calculated with Eq. (4), and the proportion of isotopically non-enriched tissue φ determined from anatomical measurements. $\Delta^{18}O_N$ is the measured difference between $\delta^{18}O_N$ and $\delta^{18}O_{soil\ 20\ cm}$, and $\Delta^{18}O_{CG}$ is calculated according to Eq. (2) and $\Delta^{18}O_{full\ model}$ according to Eq. (7).

Parameter	Drought-stressed	Irrigated
ε^+ (‰)	8.94	8.82
ε_k (‰)	28	28
D (m^2 s^{-1})	2.53e−09	2.62e−09
L (m)	0.32	0.05
E (mmol m^{-2} s^{-1})	0.28	0.55
EL (mmol m^{-1} s^{-1})	0.09	0.03
$\wp$	0.63	0.19
φ	0.27	0.28
$\delta^{18}O_{soil\ 20\ cm}$ (‰)	−6.84	−9.43
$\delta^{18}O_N$ (‰)	5.99	6.90
$\Delta^{18}O_N$ (‰)	12.83	16.33
$\Delta^{18}O_{CG}$ (‰)	23.31	24.76
$\Delta^{18}O_{full\ model}$ (‰)	12.62	16.15

differences until the 1970s. After the 1970s, however, the records started to significantly deviate and remained lower for the now-dead trees until their death compared with the living trees (Figure 4b, Student's t-test for differences between groups, 1900–59: 0.130 ± 0.118 (mean difference $\pm$ SD), n.s.; 1960–2005: -0.786 ± 0.171, $P < 0.001$). Correlation
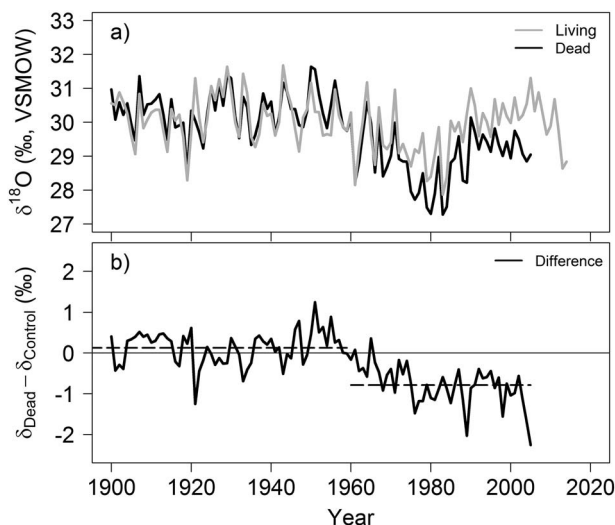
Figure 4. Tree-ring $\delta^{18}O$ chronologies of living and now-dead trees (a) and their differences (b). The dashed lines indicate the mean of the differences between dead and living for 1900–59 and 1960–2005, respectively. Note: the chronology of the dead trees covers the period 1900–2005.

Figure 5. Pearson's correlation coefficients between $\delta^{18}O$ chronologies and climate variables (T, mean temperature; P, precipitation amount; SPEI, Standardized Precipitation Evapotranspiration Index (3 m = 3 months, 6 m = 6 months); RH, relative humidity; VPD, vapor pressure deficit) for the period of 1960–2003 for spring (March–May; a) and summer (June–August; b). White bars refer to living trees and black bars to dead trees. Significant correlations are marked by * ($P < 0.05$) and ** ($P < 0.01$).

analysis between monthly climate variables and tree-ring $\delta^{18}O$ chronologies indicated the spring (March–May) and summer (June–August) seasons as most important for isotope fixation in the tree rings, and we thus focused on the correlations for these periods. Tree-ring $\delta^{18}O$ values of the living trees were positively and significantly correlated with spring temperatures and VPD (and negatively with RH), as well as with summer temperatures, precipitation amount and SPEI (Figure 5). For the now-dead trees, correlations were similar and in some cases also significant (spring VPD, summer precipitation amount and SPEI). Generally, trees that died later showed a weaker response in spring but a stronger response in summer compared with living trees (Figure 5).

Modeling of $\delta^{18}O$ in tree rings

Simulations of tree-ring $\delta^{18}O$ were performed for the time period where $\delta^{18}O$ data of precipitation are available (starting in 1972). We verified the representativeness of the precipitation $\delta^{18}O$ data as a surrogate for soil water isotopic composition by correlation analysis between measured seasonal soil water $\delta^{18}O$ of the study site (available 2013–15) and $\delta^{18}O$ of precipitation of various months. We found a highly significant correlation between soil water values of 10–20 cm depth and 2-month precipitation averages (using the current and the preceding month; $r^2 = 0.70$, $\delta^{18}O_{SW} = 0.8514 * \delta^{18}O_{precipitation} + 1.679$). This relationship was used to estimate the isotopic composition of soil water available for the trees during the growing season over the extended period of 1972–2014. Other model parameters were used as determined above for the drought-stressed trees,
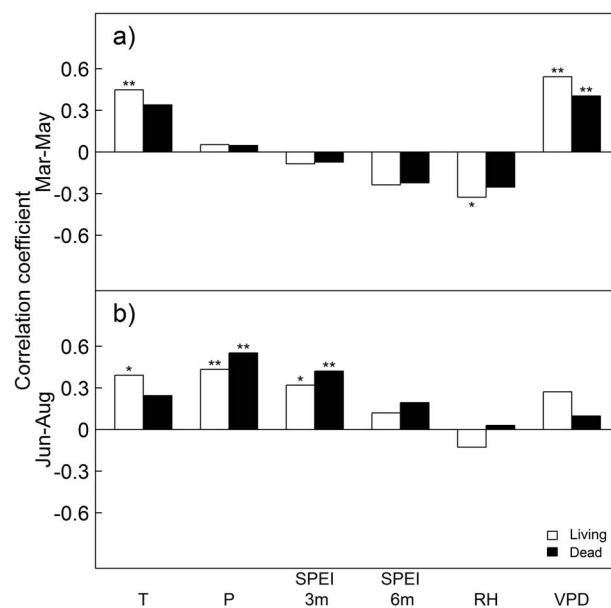
including the relationship between E and VPD to estimate past variations in E.

The correlation between measured and modeled tree-ring $\delta^{18}O$ values was significant when using the basic tree-ring CG model (Eq. (8)) for dying and surviving trees (living trees: slope = 0.31, $R^2 = 0.33$, $P < 0.001$; dead trees: slope = 0.32, $R^2 = 0.38$, $P < 0.001$), although the slopes deviated strongly from 1 and the estimated values were too high by several per mil (Figure 6). Applying the full model with the Péclet and two-pool corrections in Eq. (8), simulated values were in better agreement with measurements regarding both the absolute level and the temporal variability (Figure 6, living trees: slope = 0.38, $R^2 = 0.35$, $P < 0.001$; dead trees: slope = 0.39, $R^2 = 0.41$, $P < 0.001$). Using a range of values for L, based on the value obtained from the first experiment for drought-stressed trees ($L = 0.32$ m $\pm$ 0.16 m), shows the effect of this parameter on the tree-ring model results (Figure 6). A higher L of 0.15 m for later dying trees compared with survivors would be consistent with the observed average tree-ring $\delta^{18}O$ difference (0.79‰) between the two groups. Furthermore, we attempted to explain the remaining differences between modeled values for this range of L and data by varying x in Eq. (8). Accordingly, we found a range of $x = 0.24$–0.37 for living trees and a slightly higher range of $x = 0.31$–0.43 for dead trees.
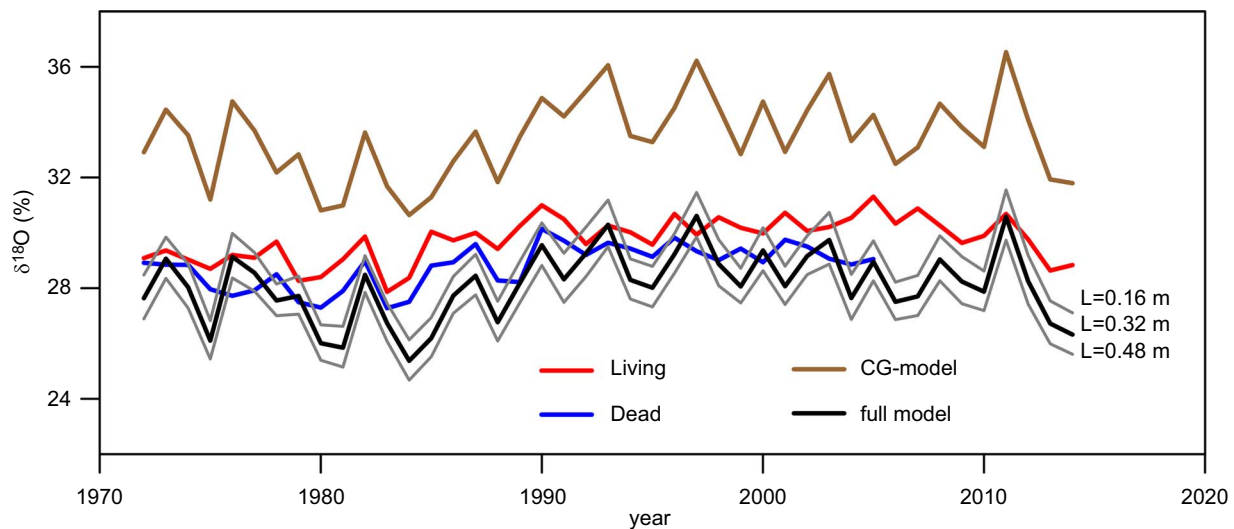
Figure 6. Time series of observed (living/now-dead) and predicted tree-ring cellulose $\delta^{18}O$ values using the basic and the full CG model with the Péclet and two-pool corrections (Eq. (8)). The effect of varying L in the full model is also shown.

Discussion

Comparison of measured and modeled needle water ^{18}O enrichment

In our first experiment on the seasonal variations in $\delta^{18}O$ of different water pools, the estimated ^{18}O enrichment using the CG model was too high for both drought-stressed and irrigated trees compared with observations of $\Delta^{18}O$, as often found in other studies (Cernusak et al. 2016), showing the need for a physiological correction. We also observed lower needle water ^{18}O enrichment for the drought-stressed compared with the irrigated trees that could not be explained by the basic CG model but by the full model considering the Péclet and two-pool corrections. The Péclet number $\wp$ is driven primarily by transpiration (E) and effective path length (L) and was shown to depend on water content and needle anatomical traits (Liang et al. 2018). Under drought stress, transpiration often decreases due to lower stomatal conductance, as also observed at our site, which would reduce $\wp$ if L is unchanged (Eqs (4) and (5)). Accordingly, needle water would be less diluted by refilling with xylem water, and therefore higher needle $\Delta^{18}O$ values could be expected under drought stress, whereas an unconstrained water supply and low VPD would result in lower needle $\Delta^{18}O$ values. This was indeed observed in some studies (Yakir et al. 1990, Roden and Ehleringer 1999), but not in our case. However, $\wp$ depends also on the effective length of the water path within the leaf or needle, which can be affected by leaf/needle morphophysiological changes under drought as well (Kahmen et al. 2008, Ferrio et al. 2012). Our results are therefore consistent assuming higher L for drought-stressed needles.

For deciduous plants, L can be estimated reasonably well (Kahmen et al. 2009), but for conifers, estimating L is often challenging, mostly due to the varying structure of a needle,

its low conductance, and generally low transpiration. Very high estimates of more than 1 m for L have previously been reported for various coniferous species, including pine (Song et al. 2013). Such values seem unrealistically high compared with the actual needle length but could be related to the tortuosity of the water path and reduced hydraulic conductivity due to the xeromorphic structure of the needle. In gymnosperms, hydraulic connections between the xylem and the mesophyll are weak, and the endodermis provides a hydraulic separation between the vascular strand and the rest of the needle (Zwieniecki et al. 2007).

By considering the two-pool model as in the full model, the Péclet correction is applied to the ^{18}O-enriched portion of needle water only, and L is thus reduced (Holloway-Phillips et al. 2016). The two-pool model was originally proposed more than two decades ago (Yakir et al. 1990, Gat and Bowser 1991), but it has only recently been revived with the expectation that it may be superior to the Péclet model (Song et al. 2015, Bögelein et al. 2017). The advantage of the two-pool model is that its parameters are more easily accessible to direct observation. The model was found to explain well, e.g., the different ^{18}O enrichment in old compared with young needles (Roden et al. 2015). When the proportion of the mesophyll tissue surrounding the needle xylem is relatively small (high φ value), the needle water signal will be strongly dominated by the unenriched xylem water, resulting in low $\Delta^{18}O$ according to the two-pool model. In our study, needle length of the drought-stressed trees was significantly lower than those of the irrigated ones. However, based on anatomical measurements, the calculated proportions of unenriched to enriched tissue did not change significantly (Table 3). This shows that needle shrinkage, i.e., the lower total cross-sectional area of the drought-stressed needles, was a result of smaller dimensions of all needle tissues. Our results

and particularly the difference between irrigated and drought-stressed trees can therefore not be explained by the two-pool model alone, but its consideration is still important for proper application of the Péclet model.

One implicit assumption in the leaf models is the isotopic equilibrium between soil water and water vapor. This may not always be true, particularly under dry conditions, owing to soil evaporation effects (Ueta et al. 2013, Bögelein et al. 2017). There could also be a difference in relative humidity or $\delta^{18}O_v$ between drought-stressed and irrigated plots. We think, however, that such influence of added water to the soil is rapidly diluted in the air at 10–12 m of canopy height. Furthermore, it is crucial to use representative source water $\delta^{18}O$ values for modeling, particularly considering root distribution and isotopic gradients at different depths (Treydte et al. 2014, Saurer et al. 2016). Uncertainties regarding the soil depth from which trees take up water tend to be large. We used $\delta^{18}O$ values from the lower soil depth (10–20 cm), rather than values from the top layer, which were ^{18}O enriched due to evaporation from the soil surface. However, even when using the topsoil water values as the source, calculated needle water ^{18}O enrichment of the drought-stressed trees was still lower than the one of the irrigated trees. In addition, the $\delta^{18}O$ soil water values down to 80 cm determined from soil excavation did not show strong deviations compared with those from 20 cm, suggesting that the source water values we used are likely to be appropriate.

Overall, the irrigation experiment enabled us to disentangle the effects of drought on needle-level oxygen isotope fractionation in mature trees, and we captured the important seasonal driving factors of needle water isotopic fractionation at our study site. This is an important prerequisite for understanding the tree-ring $\delta^{18}O$ values.

Tree-ring $\delta^{18}O$ variations in living and now-dead trees

The tree-ring $\delta^{18}O$ values of the individual living and now-dead trees as well as the means of the two groups featured very strong common variability (Figures 4a and see Figures S3 and S4 available at Supplementary Data at *Tree Physiology* Online). Our correlation analysis suggested that mainly spring mean temperature and VPD were responsible for the common $\delta^{18}O$ variations of both groups, consistent with earlier studies (Treydte et al. 2007, 2014, Giuggiola et al. 2016). This can be explained by the effect of high temperatures on the isotope ratios of precipitation and source water (Dansgaard 1964) and by the higher foliar water ^{18}O enrichment under dry conditions (Roden and Ehleringer 1999), in general agreement with the factors known to influence oxygen isotope fractionations (Eq. (8)). It is also consistent with the occurrence of frequent droughts in the studied region (Bigler et al. 2006, Rigling et al. 2013). However, dead trees were more depleted in $\delta^{18}O$ compared with the surviving trees after the 1970s (Figure 4b). This indicates that climate alone cannot explain the isotope variability but some site-specific soil or plant physiological differences must exist between the tree groups. The results from our seasonal water samples suggested that ^{18}O enrichment in drought-stressed trees was generally lower compared with that in the irrigated trees, owing to changes in needle morphology. This fits well to the lower tree-ring isotope values of the now-dead (i.e., more stressed) trees compared with the survivors. The lower needle water ^{18}O enrichment was related to higher effective path length L in drought-stressed trees, and it could therefore be possible that such a signal is recorded in the tree rings. This hypothesis will be further discussed in the modeling section below.

However, a direct mechanistic link between needle-level and stem-level signals is difficult to establish. Lower tree-ring $\delta^{18}O$ values in declining trees could also be related to seasonal differences in the use of carbohydrates (Sarris et al. 2013). Drought-stressed trees react more sensitively to favorable spring and early summer environmental conditions and therefore rely more on isotopically depleted source water from winter and spring. Tree rings may therefore reflect the isotopic signature of carbohydrates produced during the earlier part of the growing season rather than during very dry conditions in summer (Sarris et al. 2013, Pflug et al. 2015). Furthermore, lower tree-ring $\delta^{18}O$ values in stressed trees may be related to different rooting patterns and associated changes in depth of the water source compared with more healthy trees (Volkmann et al. 2016, Brinkmann et al. 2019). However, this is unlikely at our site, as the lower values would imply deeper roots of the later dying trees. This would be unexpected for already weakened trees.

Long-term differences in gas exchange between dying and surviving trees are indicated by a tree-ring study based on carbon isotopes at the same site (Timofeeva et al. 2017). The authors found that individuals with the most isohydric strategy were most prone to suffer as a result of long-term reduced carbon uptake (Timofeeva et al. 2017). As atmospheric moisture demand has been increasing during recent decades due to higher temperatures and more frequent drought (Rebetez and Dobbertin 2004), Scots pine trees tended to close their stomata and strongly reduced transpiration—potentially already for many decades at our study site. This does not, however, need to be the case on the verge of death, as dying Scots pines in Spain transpired even more than healthy individuals (Salmon et al. 2015). More insights into causes of the tree-ring isotope variations could be expected by the use of the isotope fractionation model.

Tree-ring isotope model

We applied isotope fractionation models only over the period where isotope data of precipitation were available (1972–2014). Nevertheless, the availability of such a long precipitation $\delta^{18}O$ record is precious and restricted to only a few sites globally. Modeling of $\delta^{18}O$ variations in tree-ring cellulose is more

challenging (Roden et al. 2000, Saurer et al. 2012, Treydte et al. 2014) than modeling of changes in leaf/needle water $\delta^{18}O$ values (Barbour 2007, Cernusak et al. 2016). Besides the problem of the unknown source water isotope variability, including uncertainty about the seasonal distribution of precipitation in the soil, the transfer of the isotope signal from leaf water to organic compounds in leaves such as sucrose and later cellulose is complex and involves isotope fractionation at various steps (Gessler et al. 2014, Treydte et al. 2014). Fractionations may occur because of the use of stored carbohydrates or during phloem loading and transport, but the strongest modifications are observed during cellulose formation due to exchange of carbonyl groups with xylem water, thus diluting the leaf isotope signal (Sternberg et al. 1986, Lehmann et al. 2017). Therefore, previous studies faced challenges in extracting a leaf physiological signal from tree-ring cellulose/wood $\delta^{18}O$ variations (Ogée et al. 2009, Treydte et al. 2014).

In our study, tree-ring cellulose $\delta^{18}O$ values estimated with the basic CG model were too high. However, applying the full model with an optimized Péclet path length (L) correction for each group of trees (Eq. (8)) strongly improved the agreement between data and model. The L values obtained were higher for the later dying trees ($L = 0.48$ m) compared with surviving trees ($L = 0.16$ m), consistent with lower transpiration rates for the more stressed trees. These values are in similar range as those obtained from modeling the seasonal needle data ($L = 0.32$ m vs 0.05 m). However, other model parameters could also differ between the groups of trees, notably the proportion x of isotope exchange with xylem water during cellulose formation (Song et al. 2014, Cheesman and Cernusak 2017). In a study with eucalyptus trees in Australia, x was estimated to range from 0.21 to 0.68 and increase with increasing site aridity (Cheesman and Cernusak 2017). Based on a functional link between x and the turnover of non-structural carbohydrates (Song et al. 2014), this would suggest high cycling of triose phosphates in stem tissues in dry environments, although in Song et al. (2014) the change of x with precipitation amount was not significant. In our study, we find relatively low values, which are, however, not far from the generally assumed $x = 0.42$ for heterotrophic cellulose synthesis from sucrose. Values are slightly higher for later dying, i.e., more stressed trees (0.31–0.43), compared with living trees (0.24–0.37), which would be consistent with a higher turnover of non-structural carbohydrates in stem tissues. This makes sense in a carbon-limited situation as a small sucrose pool is turned over quickly during cellulose synthesis with less opportunity for hexose phosphates to cycle through triose.

Conclusions

A combination of observed data and model simulations enabled us to derive valuable information on past tree physiological changes at our site. Interestingly, lower $\delta^{18}O$ values were also observed for declining Norway spruce (*Picea abies* L. Karst.) at two sites in Norway (Hentschel et al. 2014). In this study, the authors concluded that such behavior may be due to changes in anatomical and physiological traits of trees under drought conditions, which could be examined to infer the risk of future tree decline. Therefore, such changes and related isotope traces under drought could be common for conifers, and $\delta^{18}O$ may be helpful for estimating the 'health status' of trees, particularly in combination with $\delta^{13}C$ (Scheidegger et al. 2000, Gessler et al. 2018). Our results are among the first demonstrating that needle-level changes in ^{18}O enrichment of trees exposed to long-term drought could be reflected in the $\delta^{18}O$ variations of tree rings. This method can potentially be applied either for retrospectively analyzing past tree physiological changes or even to predict decline and/or mortality of vulnerable trees.

Conflict of interest

None declared.

References

Aguadé D, Poyatos R, Rosas T, Martínez-Vilalta J (2015) Comparative drought responses of *Quercus ilex* L. and *Pinus sylvestris* L. in a montane forest undergoing a vegetation shift. Forests 6:2505–2529.

Allen CD, Macalady AK, Chenchouni H et al. (2010) A global overview of drought and heat-induced tree mortality reveals emerging climate change risks for forests. For Ecol Manage 259:660–684.

Allen CD, Breshears DD, McDowell NG (2015) On underestimation of global vulnerability to tree mortality and forest die-off from hotter drought in the Anthropocene. Ecosphere 6:1–55.

Anderegg WRL, Kane JM, Anderegg LDL (2013) Consequences of widespread tree mortality triggered by drought and temperature stress. Nat Clim Chang 3:30–36.

Barbour MM (2007) Stable oxygen isotope composition of plant tissue: a review. Funct Plant Biol 34:83–94.

Barbour MM, Roden JS, Farquhar GD, Ehleringer JR (2004) Expressing leaf water and cellulose oxygen isotope ratios as enrichment above source water reveals evidence of a Péclet effect. Oecologia 138:426–435.

Bigler C, Bräker OU, Bugmann H, Dobbertin M, Rigling A (2006) Drought as an inciting mortality factor in scots pine stands of the Valais, Switzerland. Ecosystems 9:330–343.

Boettger T, Haupt M, Knöller K et al. (2007) Wood cellulose preparation methods and mass spectrometric analyses of δ^{13}C, δ^{18}O, and nonexchangeable δ^2H values in cellulose, sugar, and starch: an interlaboratory comparison. Anal Chem 79:4603–4612.

Bögelein R, Thomas FM, Kahmen A (2017) Leaf water ^{18}O and ^{2}H enrichment along vertical canopy profiles in a broadleaved and a conifer forest tree. Plant Cell Environ. 40:1086–1103.

Bottinga Y, Craig H (1968) Oxygen isotope fractionation between CO_2 and water, and the isotopic composition of marine atmospheric CO_2. Earth Planet Sci Lett 5:285–295.

Breshears DD, Adams HD, Eamus D, McDowell NG, Law DJ, Will RE, Williams AP, Zou CB (2013) The critical amplifying role of increasing atmospheric moisture demand on tree mortality and associated regional die-off. Front Plant Sci 4:266.

Brinkmann N, Eugster W, Buchmann N, Kahmen A (2019) Species-specific differences in water uptake depth of mature temperate trees vary with water availability in the soil. Plant Biol 21:71–81.

Cernusak LA, Barbour MM, Arndt SK et al. (2016) Stable isotopes in leaf water of terrestrial plants. Plant Cell Environ 39:1087–1102.

Cheesman AW, Cernusak LA (2017) Infidelity in the outback: climate signal recorded in Δ^{18}O of leaf but not branch cellulose of eucalypts across an Australian aridity gradient. Tree Physiol 37:554–564.

Choat B, Jansen S, Brodribb TJ et al. (2012) Global convergence in the vulnerability of forests to drought. Nature 491:752–755.

Cocozza C, de Miguel M, Pšidová E et al. (2016) Variation in ecophysiological traits and drought tolerance of beech (*Fagus sylvatica* L.) seedlings from different populations. Front Plant Sci 7:886.

Craig H, Gordon LI (1965) Deuterium and oxygen 18 variations in the ocean and the marine atmosphere. Consiglio nazionale delle richerche, Laboratorio de geologia nucleare, Pisa.

Cuntz M, Ogée J, Farquhar GD, Peylin P, Cernusak LA (2007) Modelling advection and diffusion of water isotopologues in leaves. Plant Cell Environ 30:892–909.

Dansgaard W (1964) Stable isotopes in precipitation. Tellus 16:436–468.

Dawdy DR (1964) Statistical and probability analysis of hydrologic data, part III: analysis of variance, covariance and time series. In: Te, Chow V (ed) Handbook of Applied Hydrology, McGraw-Hill, New York, pp 868–890.

DeNiro MJ, Epstein S (1981) Isotopic composition of cellulose from aquatic organisms. Geochim Cosmochim Acta 45:1885–1894.

Dobbertin M, Eilmann B, Bleuler P, Giuggiola A, Pannatier EG, Landolt W, Schleppi P, Rigling A (2010) Effect of irrigation on needle morphology, shoot and stem growth in a drought-exposed *Pinus sylvestris* forest. Tree Physiol 30:346–360.

Dongmann G, Nürnberg HW, Förstel H, Wagener K (1974) On the enrichment of $H_2{}^{18}$O in the leaves of transpiring plants. Radiat Environ Biophys 11:41–52.

Duan H, O'Grady AP, Duursma RA, Choat B, Huang G, Smith RA, Jiang Y, Tissue DT (2015) Drought responses of two gymnosperm species with contrasting stomatal regulation strategies under elevated [CO_2] and temperature. Tree Physiol 35:756–770.

Edwards TWD, Birks SJ, Luckman BH, MacDonald GM (2008) Climatic and hydrologic variability during the past millennium in the eastern Rocky Mountains and northern Great Plains of western Canada. Quat Res 70:188–197.

Ehleringer JR, Dawson TE (1992) Water uptake by plants: perspectives from stable isotope composition. Plant Cell Environ 15: 1073–1082.

Eilmann B, Buchmann N, Siegwolf R, Saurer M, Cherubini P, Rigling A (2010) Fast response of scots pine to improved water availability reflected in tree-ring width and δ^{13}C. Plant Cell Environ 33:1351–1360.

Farquhar GD, Lloyd J (1993) Carbon and oxygen isotope effects in the exchange of carbon dioxide between terrestrial plants and the atmosphere. In: Ehleringer JR, Hall AE, Farquhar GD (eds) Stable isotopes and plant carbon-water relations. Academic Press, San Diego, CA, pp 47–70.

Farquhar GD, Cernusak LA, Barnes B (2007) Heavy water fractionation during transpiration. Plant Physiol 143:11–18.

Ferrio JP, Pou A, Florez-Sarasa I, Gessler A, Kodama N, Flexas J, Ribas-Carbó M (2012) The Péclet effect on leaf water enrichment correlates with leaf hydraulic conductance and mesophyll conductance for CO_2. Plant Cell Environ 35:611–625.

Fleck S, Raspe S, Cater M et al. (2016) Part XVII: leaf area measurements. In: UNECE ICP Forests Programme Co-ordinating Centre (ed) Manual on methods and criteria for harmonized sampling, assessment, monitoring and analysis of the effects of air pollution on forests. Thünen Institute of Forest Ecosystems, Eberswalde, Germany, p 44.

Foerstel H, Huetzen H (1983) ^{18}O/^{16}O Ratio of Water in a Local Ecosystem as a Basis of Climate Record. IAEA, International Atomic Energy Agency, Vienna.

Galiano L, Martínez-Vilalta J, Lloret F (2010) Drought-induced multi-factor decline of scots pine in the pyrenees and potential vegetation change by the expansion of co-occurring oak species. Ecosystems 13:978–991.

Galle A, Esper J, Feller U, Ribas-Carbo M, Fonti P (2010) Responses of wood anatomy and carbon isotope composition of *Quercus pubescens* saplings subjected to two consecutive years of summer drought. Ann Forest Sci 67:809–809.

Gat JR, Bowser C (1991) The heavy isotope enrichment of water in coupled evaporative systems. In: Taylor HP Jr, O'Neil JR, Kaplan IR (eds) Stable isotope geochemistry: a tribute to Samuel Epstein Geochemical Society.

Gaylord ML, Kolb TE, McDowell NG (2015) Mechanisms of piñon pine mortality after severe drought: a retrospective study of mature trees. Tree Physiol 35:806–816.

Gessler A, Brandes E, Buchmann N, Helle G, Rennenberg H, Barnard RL (2009) Tracing carbon and oxygen isotope signals from newly assimilated sugars in the leaves to the tree-ring archive. Plant Cell Environ 32:780–795.

Gessler A, Ferrio JP, Hommel R, Treydte K, Werner RA, Monson RK (2014) Stable isotopes in tree rings: towards a mechanistic

understanding of isotope fractionation and mixing processes from the leaves to the wood. Tree Physiol 34:796–818.

Gessler A, Cailleret M, Joseph J et al. (2018) Drought induced tree mortality—a tree-ring isotope based conceptual model to assess mechanisms and predispositions. New Phytol 219:485–490.

Giuggiola A, Ogée J, Rigling A, Gessler A, Bugmann H, Treydte K (2016) Improvement of water and light availability after thinning at a xeric site: which matters more? A dual isotope approach. New Phytol 210:108–121.

Grossiord C, Sevanto S, Limousin JM et al. (2018) Manipulative experiments demonstrate how long-term soil moisture changes alter controls of plant water use. Environ Exp Bot 152:19–27.

Hentschel R, Rosner S, Kayler ZE, Andreassen K, Børja I, Solberg S, Tveito OE, Priesack E, Gessler A (2014) Norway spruce physiological and anatomical predisposition to dieback. For Ecol Manage 322:27–36.

Herzog C, Steffen J, Graf Pannatier E, Hajdas I, Brunner I (2014) Nine years of irrigation cause vegetation and fine root shifts in a water-limited pine Forest. PLoS One 9:e96321.

Holloway-Phillips M, Cernusak LA, Barbour M, Song X, Cheesman A, Munksgaard N, Stuart-Williams H, Farquhar GD (2016) Leaf vein fraction influences the Péclet effect and ^{18}O enrichment in leaf water. Plant Cell Environ 39:2414–2427.

Kahmen A, Simonin K, Tu KP, Merchant A, Callister A, Siegwolf R, Dawson TE, Arndt SK (2008) Effects of environmental parameters, leaf physiological properties and leaf water relations on leaf water $\delta^{18}O$ enrichment in different eucalyptus species. Plant Cell Environ 31:738–751.

Kahmen A, Simonin K, Tu K, Goldsmith GR, Dawson TE (2009) The influence of species and growing conditions on the 18-O enrichment of leaf water and its impact on 'effective path length'. New Phytol 184:619–630.

Labuhn I, Daux V, Girardclos O, Stievenard M, Pierre M, Masson-Delmotte V (2016) French summer droughts since 1326 CE: a reconstruction based on tree ring cellulose $\delta^{18}O$. Clim Past 12:1101–1117.

Laumer W, Andreu L, Helle G, Schleser GH, Wieloch T, Wissel H (2009) A novel approach for the homogenization of cellulose to use micro-amounts for stable isotope analyses. Rapid Commun Mass Spectrom 23:1934–1940.

Leavitt SW, Danzer SR (1993) Method for batch processing small wood samples to holocellulose for stable-carbon isotope analysis. Anal Chem 65:87–89.

Lehmann MM, Gamarra B, Kahmen A, Siegwolf RTW, Saurer M (2017) Oxygen isotope fractionations across individual leaf carbohydrates in grass and tree species. Plant Cell Environ 40:1658–1670.

Liang J, Wright JS, Cui XW, Sternberg L, Gan WX, Lin GH (2018) Leaf anatomical traits determine the O-18 enrichment of leaf water in coastal halophytes. Plant Cell Environ 41:2744–2757.

Libby LM, Pandolfi LJ, Payton PH, Marshall J, Becker B, Giertz-Sienbenlist V (1976) Isotopic tree thermometers. Nature 261:284–288.

Masson-Delmotte V, Raffalli-Delerce G, Danis PA et al. (2005) Changes in European precipitation seasonality and in drought frequencies revealed by a four-century-long tree-ring isotopic record from Brittany, western France. Clim Dyn 24:57–69.

McCarroll D, Loader NJ (2004) Stable isotopes in tree rings. Quat Sci Rev 23:771–801.

McDowell NG, Pockman WT, Allen CD et al. (2008) Mechanisms of plant survival and mortality during drought: why do some plants survive while others succumb to drought? New Phytol 178:719–739.

Moreno-Gutiérrez C, Dawson TE, Nicolás E, Querejeta JI (2012) Isotopes reveal contrasting water use strategies among coexisting plant species in a Mediterranean ecosystem. New Phytol 196:489–496.

Ogée J, Cuntz M, Peylin P, Bariac T (2007) Non-steady-state, non-uniform transpiration rate and leaf anatomy effects on the progressive stable isotope enrichment of leaf water along monocot leaves. Plant Cell Environ 30:367–387.

Ogée J, Barbour MM, Wingate L et al. (2009) A single-substrate model to interpret intra-annual stable isotope signals in tree-ring cellulose. Plant Cell Environ 32:1071–1090.

Pearson M, Saarinen M, Nummelin L, Heiskanen J, Roitto M, Sarjala T, Laine J (2013) Tolerance of peat-grown scots pine seedlings to waterlogging and drought: morphological, physiological, and metabolic responses to stress. For Ecol Manage 307:43–53.

Pflug EE, Siegwolf R, Buchmann N, Dobbertin M, Kuster TM, Günthardt-Goerg MS, Arend M (2015) Growth cessation uncouples isotopic signals in leaves and tree rings of drought-exposed oak trees. Tree Physiol 35:1095–1105.

Poyatos R, Aguadé D, Galiano L, Mencuccini M, Martínez-Vilalta J (2013) Drought-induced defoliation and long periods of near-zero gas exchange play a key role in accentuating metabolic decline of scots pine. New Phytol 200:388–401.

Rebetez M, Dobbertin M (2004) Climate change may already threaten scots pine stands in the Swiss alps. Theor Appl Climatol 79:1–9.

Rigling A, Bigler C, Eilmann B et al. (2013) Driving factors of a vegetation shift from scots pine to pubescent oak in dry Alpine forests. Glob Chang Biol 19:229–240.

Rinne KT, Loader NJ, Switsur VR, Waterhouse JS (2013) 400-year May–August precipitation reconstruction for southern England using oxygen isotopes in tree rings. Quat Sci Rev 60:13–25.

Roden J, Kahmen A, Buchmann N, Siegwolf R (2015) The enigma of effective path length for ^{18}O enrichment in leaf water of conifers. Plant Cell Environ 38:2551–2565.

Roden JS, Ehleringer JR (1999) Observations of hydrogen and oxygen isotopes in leaf water confirm the Craig-Gordon model under wide-ranging environmental conditions. Plant Physiol 120:1165–1174.

Roden JS, Johnstone JA, Dawson TE (2009) Intra-annual variation in the stable oxygen and carbon isotope ratios of cellulose in tree rings of coast redwood (Sequoia sempervirens). Holocene 19:189–197.

Roden JS, Lin G, Ehleringer JR (2000) A mechanistic model for interpretation of hydrogen and oxygen isotope ratios in tree-ring cellulose. Geochim Cosmochim Acta 64:21–35.

Rowland L, da Costa ACL, Galbraith DR et al. (2015) Death from drought in tropical forests is triggered by hydraulics not carbon starvation. Nature 528:119–122.

Salmon Y, Torres-Ruiz JM, Poyatos R, Martinez-Vilalta J, Meir P, Cochard H, Mencuccini M (2015) Balancing the risks of hydraulic failure and carbon starvation: a twig scale analysis in declining Scots pine. Plant Cell Environ 38:2575–2588.

Sargeant CI, Singer MB (2016) Sub-annual variability in historical water source use by Mediterranean riparian trees. Ecohydrology 9:1328–1345.

Sarris D, Siegwolf R, Körner C (2013) Inter- and intra-annual stable carbon and oxygen isotope signals in response to drought in Mediterranean pines. Agric For Meteorol 168:59–68.

Saurer M, Aellen K, Siegwolf R (1997) Correlating $\delta^{13}C$ and $\delta^{18}O$ in cellulose of trees. Plant Cell Environ 20:1543–1550.

Saurer M, Kress A, Leuenberger M, Rinne KT, Treydte KS, Siegwolf RTW (2012) Influence of atmospheric circulation patterns on the oxygen isotope ratio of tree rings in the alpine region. J Geophys Res Atmos 117:2156–2202.

Saurer M, Kirdyanov AV, Prokushkin AS, Rinne KT, Siegwolf RTW (2016) The impact of an inverse climate–isotope relationship in soil water on the oxygen-isotope composition of Larix gmelinii in Siberia. New Phytol 209:955–964.

Scheidegger Y, Saurer M, Bahn M, Siegwolf R (2000) Linking stable oxygen and carbon isotopes with stomatal conductance and photosynthetic capacity: a conceptual model. Oecologia 125: 350–357.

Song X, Farquhar GD, Gessler A, Barbour MM (2014) Turnover time of the non-structural carbohydrate pool influences $\delta^{18}O$ of leaf cellulose. Plant Cell Environ 37:2500–2507.

Song X, Loucos KE, Simonin KA, Farquhar GD, Barbour MM (2015) Measurements of transpiration isotopologues and leaf water to assess enrichment models in cotton. New Phytol 206:637–646.

Song XIN, Barbour MM, Farquhar GD, Vann DR, Helliker BR (2013) Transpiration rate relates to within- and across-species variations in effective path length in a leaf water model of oxygen isotope enrichment. Plant Cell Environ 36:1338–1351.

Sternberg L (2009) Oxygen stable isotope ratios of tree-ring cellulose: the next phase of understanding. New Phytol 181:553–562.

Sternberg L, Deniro MJ, Savidge RA (1986) Oxygen isotope exchange between metabolites and water during biochemical reactions leading to cellulose synthesis. Plant Physiol 82:423–427.

Timofeeva G, Treydte K, Bugmann H, Rigling A, Schaub M, Siegwolf R, Saurer M (2017) Long-term effects of drought on tree-ring growth and carbon isotope variability in scots pine in a dry environment. Tree Physiol 37:1028–1041.

Treydte K, Frank D, Esper J et al. (2007) Signal strength and climate calibration of a European tree-ring isotope network. Geophys Res Lett 34:L24302.

Treydte K, Boda S, Graf Pannatier E et al. (2014) Seasonal transfer of oxygen isotopes from precipitation and soil to the tree ring: source water versus needle water enrichment. New Phytol 202:772–783.

Treydte KS, Schleser GH, Helle G, Frank DC, Winiger M, Haug GH, Esper J (2006) The twentieth century was the wettest period in northern Pakistan over the past millennium. Nature 440:1179–1182.

Ueta A, Sugimoto A, Iijima Y, Yabuki H, Maximov TC, Velivetskaya TA, Ignatiev AV (2013) Factors controlling diurnal variation in the isotopic composition of atmospheric water vapour observed in the taiga, eastern Siberia. Hydrol Process 27:2295–2305.

Volkmann THM, Haberer K, Gessler A, Weiler M (2016) High-resolution isotope measurements resolve rapid ecohydrological dynamics at the soil-plant interface. New Phytol 210:839–849.

Waterhouse JS, Switsur VR, Barker AC, Carter AHC, Robertson I (2002) Oxygen and hydrogen isotope ratios in tree rings: how well do models predict observed values? Earth Planet Sci Lett 201: 421–430.

Weigt RB, Bräunlich S, Zimmermann L, Saurer M, Grams TEE, Dietrich H-P, Siegwolf RTW, Nikolova PS (2015) Comparison of $\delta^{18}O$ and $\delta^{13}C$ values between tree-ring whole wood and cellulose in five species growing under two different site conditions. Rapid Commun Mass Spectrom 29:2233–2244.

West AG, Patrickson SJ, Ehleringer JR (2006) Water extraction times for plant and soil materials used in stable isotope analysis. Rapid Commun Mass Spectrom 20:1317–1321.

Yakir D, DeNiro MJ, Gat JR (1990) Natural deuterium and oxygen-18 enrichment in leaf water of cotton plants grown under wet and dry conditions: evidence for water compartmentation and its dynamics. Plant Cell Environ 13:49–56.

Zwieniecki MA, Brodribb TJ, Holbrook NM (2007) Hydraulic design of leaves: insights from rehydration kinetics. Plant Cell Environ 30:910–921.